Journal of Solid State Chemistry **167,** 1–6 (2002)
doi:10.1006/jssc.2002.9590

Phase Transition from the Cubic Zintl Phase LiIn into a Tetragonal Structure at Low Temperature

Helmut Ehrenberg,*[,1] Hermann Pauly,* Thomas Hansen,† Jean-Christophe Jaud,* and Hartmut Fuess*

*Darmstadt University of Technology, Materials Science, Petersenstr. 23, D-64287 Darmstadt, Germany; and †Institut Laue-Langevin, BP 156, F-38042 Grenoble Cedex 9, France

Received December 26, 2001; received in revised form March 1, 2002; accepted March 15, 2002

The binary face-centered cubic Zintl phase LiIn (NaTl-type, B32 in the classification of the "Strukturberichte") undergoes a tetragonal distortion from $Fd\bar{3}m$ into $I4_1/amd$. This phase transition is reversible and "translationengleich". The transition temperature of 170(10) K was determined based on X-ray and neutron powder diffraction data. © 2002 Elsevier Science (USA)

Key Words: **Zintl phase; NaTl-type structure; B32; *translationengleiche* phase transitions; LiIn.**

1. INTRODUCTION

Zintl phases have attracted the attention of chemists and physicists due to their peculiar type of bonding: The generally accepted characteristics of Zintl phases is a unique hybrid bonding with covalent, metallic, and ionic contributions (1–3). Early investigations were focused on binary phases with NaTl-type structure and a discussion of the preconditions for their existence, which are only rarely satisfied (4, 5). Binary alloys composed of two different metals with not too different atomic radii and a 1:1 stoichiometry crystallize very often (more than 200 examples) in a cubic CsCl-type lattice, spacegroup $Pm\bar{3}m$, i.e., in the B2-type according to the classification scheme of the "Strukturberichte." In a few exceptional cases, such alloys crystallize in an NaTl-type structure, spacegroup $Fd\bar{3}m$, i.e., in the B32-type. Until now only seven examples are known at ambient conditions; they are called Zintl phases in a strict sense of the name. Later on, the classification of Zintl phases was extended to other structure types (1).

In both the B2- and B32-type structures, each atom is surrounded in a cubic coordination by eight atoms in the nearest-neighbor shell. The striking differences between the two structure types are the eight nearest neighbors. In the B2 lattice, all neighbors are unlike, whereas in the rare B32-lattice only four of them are unlike and the other 4 are of the same type, see Fig. 2 in (7).

More NaTl-type structures are, however, observed if ternary alloys are included. No less than 20 ternary alloys with NaTl-type structure are described (6,7).

Within a comprehensive reinvestigation of the structural peculiarities of the ternary fcc alloys of the NaTl-type even some of the seven known binary alloys with this structure have been revisited. LiIn is one of the rare binary alloys and marks the binary endpoint in the homogeneous quasibinary section $Li(Ag_xIn_{1-x})$ $(0 \le x \le 0.5)$, in which Ag and In are statistically distributed on the same crystallographic site as In in LiIn. Recently, high-pressure-induced phase transitions in LiIn and LiCd from the B32- into the B2-type at 11(1) GPa and room temperature have been reported and discussed (8). Phase transitions reveal significant information about the underlying interactions and bonding conditions as the transition reflects the crossing of at least two hyperfaces in the representation space of free energy versus configuration. γ-NaHg was established as the eighth binary Zintl phase with NaTl-type structure, but only at a high temperature (9). At ambient conditions, α-NaHg exists in a distorted CsCl-type structure, and the intermediate phase β-NaHg with distorted NaTl-type structure is observed between 165°C and 176°C. In spite of this strong hint to a stabilization of the NaTl-type structure by entropy and anomalies in the temperature dependence of physical properties of several Zintl phases (10–14), a structural investigation at a low temperature is still lacking for the seven "classical" binary Zintl phases with NaTl-type structure. In this contribution, we report on the crystal structure of LiIn between 1.5 K and room temperature, studied by X-ray and neutron powder diffraction. Further-

[1]To whom correspondence should be addressed. Fax: +49-6151-166023. E-mail: helmut@tu-darmstadt.de.

0022-4596/02 $35.00

more, the neutron diffraction data are analyzed with respect to vacancies in the Li-sublattice and their correlation with different thermal displacement parameters for the Li- and In-sites. The behavior of stoichiometric LiIn is compared with the results for samples with 3% Li-deficiency and 3% Li-excess on one hand and with $Li(Ag_{0.25}In_{0.75})$ and $Li(Ag_{0.5}In_{0.5})$ on the other.

2. EXPERIMENTAL DETAILS

All the investigated samples were prepared from the following reactants: lithium (rod of 10 mm diameter, 99.9%, Alfa Aesar), indium (ingots, 99.9999%, Alfa Aesar), and Ag wire (Degussa-Hüls AG). Appropriate amounts were mixed according to the expected stoichiometry of the product and filled into iron crucibles. Note that the crucibles should be made from unalloyed steel without any Ni or Cr. These crucibles have been sealed by welding under dry argon atmosphere, placed into the furnace, which was preheated to 1000°C, and heavily shaked to mix up the reactants properly. After 5–10 min, the samples were cooled down to room temperature rapidly by removing the crucible from the furnace into ambient conditions. The reaction product is very sensitive to moisture and had to be ground in an agate mortar within a dry glove box for further analysis by X-ray and neutron powder diffraction.

X-ray diffraction patterns were collected on an STOE STADI P, equipped with a linear position-sensitive detector with 6° aperture. A Ge(1 1 1) monochromator was used to select Co$K\alpha_1$ radiation. The sample was filled into sealed capillaries of 0.3 mm diameter and cooled by flowing nitrogen using a cryostreamer from Oxford Cryosystems. Intensities were recorded in steps of $\Delta 2\Theta = 0.02°$ for selected ranges.

Neutron powder diffraction was performed at the beamlines D2B and D20 of the Insitut Laue-Langevin in Grenoble using vanadium cylinders of 5.88 mm diameter as sample holders and an Orange Cryostat for temperature control. The neutron wavelengths were 1.5938 Å (D2B) and 1.2878 Å (D20), respectively.

The software packages GSAS (15) and Fullprof (16) were used for the Rietveld refinements of the structure models based on both X-ray and neutron diffraction data.

3. RESULTS

Neutron powder diffraction data from beamline D2B on LiIn at 2 K reveal a splitting of reflections with respect to the cubic NaTl-type structure observed at room temperature. The splitting scheme indicates a tetragonal body-centered low-temperature structure with $a_{tet} \sim a_{cub}/\sqrt{2}$ and $c_{tet} \sim c_{cub}$. Based on subgroup considerations, the space group $I4_1/amd$ with Li on the (4*a*)- and In on the (4*b*)-site is derived as a model for the crystal structure of LiIn at a low temperature. This structure model was refined based on the neutron powder diffraction data collected at beamline D2B. The excellent agreement between observed and calculated profiles confirms the proposed starting model, see Fig. 1. The evolution of the structure parameters with temperature was monitored by neutron powder diffraction at beamline D20, which allows fast data collection, although the splitting of reflections is not explicitly resolved. One hundred diffraction patterns have been recorded during cooling from room temperature down to 2 K, and the results are summarized in Fig. 2. For the stability region of the cubic room-temperature structure the lattice parameter a is plotted as $a_{cub}/\sqrt{2}$ and V as $V_{cub}/2$ for a better comparison with the tetragonal low-temperature structure. The onset of the tetragonal splitting during cooling is clearly seen by the poorer agreement between observed and calculated profiles, measured by χ^2, for a refinement based on the cubic structure model, see Fig. 2e. χ^2 increases from typical values between 1.3 and 1.4 down to 180 K to 1.8 at 150 K. However, by including the tetragonal distortion a significantly better agreement can be obtained. Based on these results, the transition temperature can be narrowed down to 160 and 180 K. This temperature region is indicated by the dashed lines. No discontinuity in the reduced cell volume is observed at the transition point, while jumps of the *a*- and *c*-parameter are obvious. The spontaneous tetragonal and temperature-independent distortion $c/(\sqrt{2}a)$ of about 0.50–0.55% indicates a first-order phase transition, which is *translationengleich*. The thermal displacement factors decrease continuously with temperature for both Li and In, but a slight hump in the transition region might give some evidence for a pronounced role of Li in the dynamics of this transition. Note that the presented values are biased by

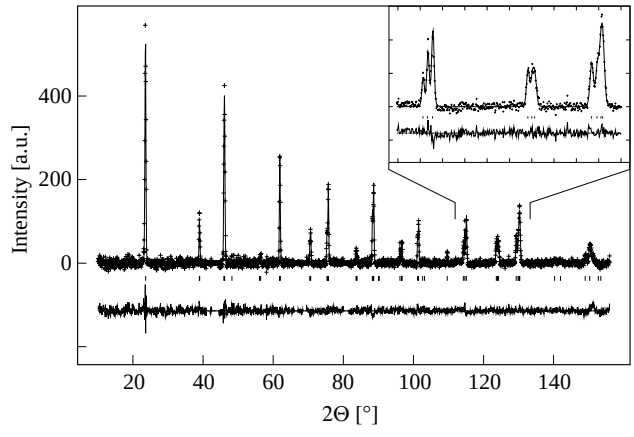

FIG. 1. Observed and calculated neutron powder diffraction patterns of LiIn at 1.5 K together with their difference curve (D2B, HR in Table 3, $R_{wp} = 6.6\%$, $R_p = 5.2\%$).

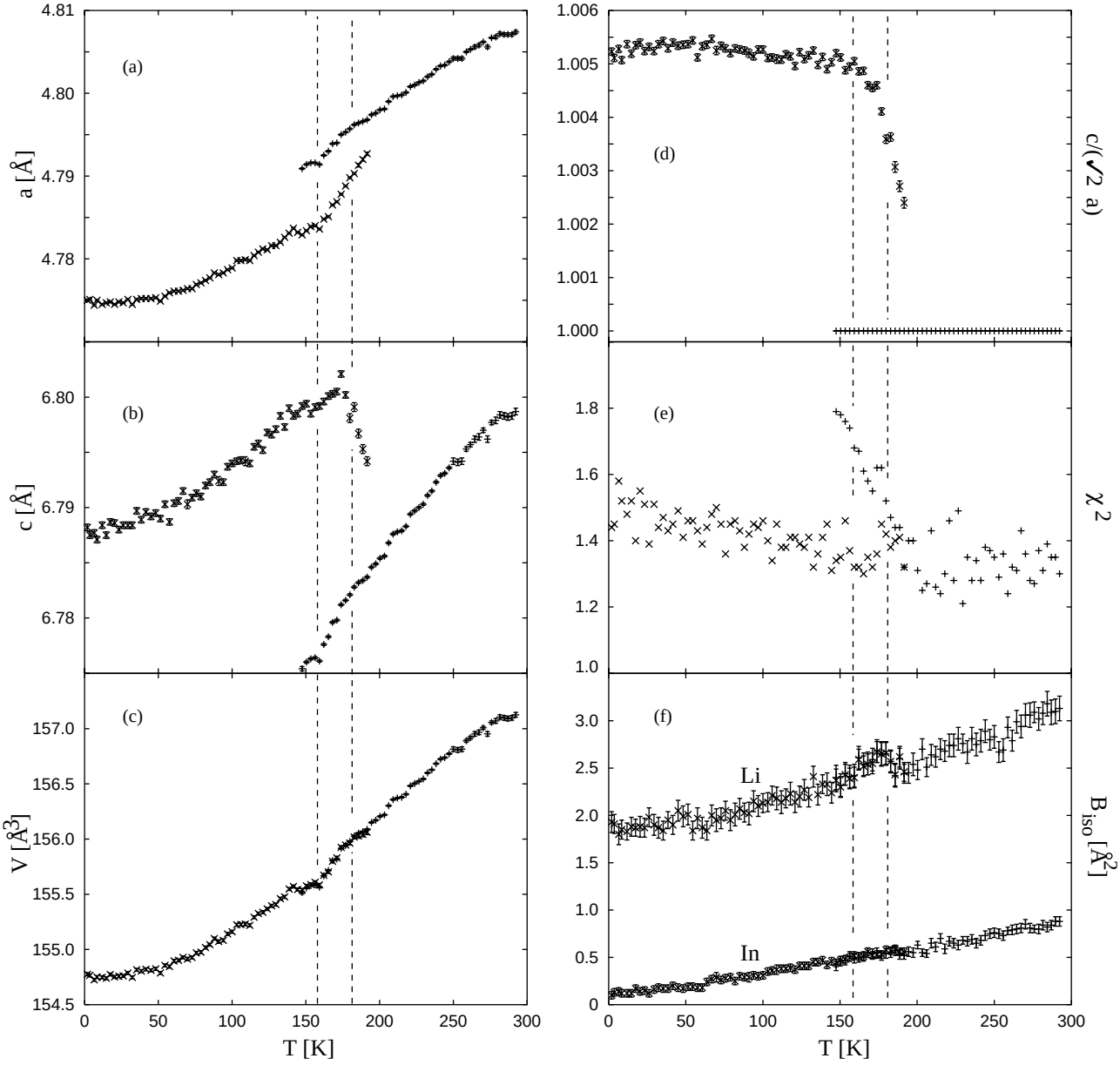

FIG. 2. Temperature dependence of the lattice parameters (a,b), unit cell volume (c), tetragonal distortion (d), agreement between observed and calculated profiles (e) and isotropic thermal displacement parameters (f) of LiIn during cooling, measured at beamline D20 of the ILL, Grenoble. "+" indicates a refinement based on the cubic room-temperature structure, "x" on the tetragonal low-temperature structure. Both models have been refined over the temperature region from 150 to 200 K for comparison.

absorption effects. The numerical correction of absorption in the D2B experiment has resulted in an increase of B_{iso} to 3.4 Å^2 for Li from 2.0 Å^2 for the uncorrected data and to 0.84 Å^2 for In from −0.4 Å^2. A similar rescaling was also made for the D20 data, but gave a less pronounced change because of the shorter neutron wavelength.

Both the transition temperature of about 170(10) K and the absolute value for the tetragonal distortion 0.50–0.55% are fully supported by the X-ray diffraction results, summarized in Table 1. The observed distortion is about 5 times larger than the detection limit of the used setup.

The cubic ↔ tetragonal phase transition is also observed for LiIn with 3% Li-deficiency, but the tetragonal distortion is slightly less pronounced and refined to only 0.45% instead of 0.50–0.55% for stoichiometric LiIn. Nevertheless, this smaller tetragonal distortion was still

TABLE 1
Lattice Parameters of LiIn at Different Temperatures as Refined Based on X-Ray Diffraction Data

T/K	a Å	c Å	$\eta = c/(\sqrt{2}a)$
250.0(1)		6.7927(3)	
220.0(1)		6.7843(3)	
180.0(1)		6.7775(4)	
170.0(1)		6.7792(5)	
160.0(1)	4.7821(5)	6.7944(10)	1.0047(3)
140.0(1)	4.7801(1)	6.7950(3)	1.0052(1)
120.0(1)	4.7783(2)	6.7919(5)	1.0051(1)
102.3(2)	4.7761(4)	6.7896(8)	1.0052(2)

sufficient to allow detection during cooling on D20 at ILL, and about the same transition temperature as for LiIn was confirmed.

The ternary alloys $LiAg_{0.25}In_{0.75}$ and $LiAg_{0.5}In_{0.5}$ are members of the solid solution in the quasibinary section LiAg–LiIn with $LiAg_{0.5}In_{0.5}$ as the endpoint. These two alloys gave no indication for a phase transition down to 2 K. Therefore, silver seems to stabilize the cubic NaTl-type structure. Note that $LiAg_{0.25}In_{0.75}$ reveals a minor and $LiAg_{0.5}In_{0.5}$ a remarkable peak-broadening as compared with LiIn. All experiments performed are summarized in Table 3 together with the key results.

4. GEOMETRICAL ASPECTS

In the tetragonal low-temperature structure, Li and In are still on crystallographic sites without any refineable positional parameter. Therefore, all effects on bond length during the phase transition scale with the tetragonal distortion $\eta = c/a\sqrt{2}$. The values for the closest three coordination shells are summarized in Table 2 from refinements using the cubic versus the tetragonal structure model, based on the neutron powder diffraction data collected at 160 K. Accordingly, the phase transition affects mainly the second coordination shell, where unlike pair distances split exactly in the ratio η. The $[LiLi_4]$- and $[LiIn_4]$-tetrahedra of the first coordination shells are slightly distorted in such a way, that the distances are not affected, but the ideal tetrahedral angle of $\alpha = 109.47^\circ$ is split into $\alpha_1 = \arccos -\eta^2/(\eta^2+2) = 109.61^\circ$ and $\alpha_2 = \arccos(\eta^2-2)/(\eta^2+2) = 109.20^\circ$.

In the cubic phase, only isotropic thermal displacement is allowed by symmetry for both sites. The reduction of symmetry due to the tetragonal distortion introduces one additional anisotropic thermal displacement parameter for each site in the low-temperature phase. However, the refinement of these two extra parameters did not result in a significant improvement between observed and calculated intensity profiles, and therefore, only isotropic thermal displacements have been considered further. Nevertheless, the isotropic thermal displacements are significantly different for Li and In. The higher values for the much lighter Li atoms are reasonable and confirmed for nearly all cubic NaTl-type-structured Zintl phases (references are given below), but the absolute values are biased by absorption, and the numerical correction is limited by the reliability of the estimated packing density of the sample in the vanadium can. The thermal displacements are also biased if Li-vacancies are included in the refinement process, and up to 10% vacancies can appear accompanied by reduced thermal displacement parameters. Li-vacancies in B32-alloys are widely discussed in the literature (often together with the extraordinary high thermal displacements of the alkali atoms) (17–24, 13, 14). The vacancies in the alkali sublattice are often confirmed by supplementary investigations of other properties. However, the structure refinements based only on powder diffraction data are not reliable due to severe correlation with the thermal displacement parameter for Li. The thermal displacement parameter for Li—or the amount of vacancies in the Li sublattice—decrease with increasing silver content in the ternary Li(In,Ag) alloys along the quasibinary section LiAg–LiIn.

TABLE 2
Changes in Atomic Distances during the Cubic ↔ Tetragonal Phase Transition in LiIn for the Closest Three Coordination Shells

	Cubic			Tetragonal			
Shell	Atoms	Distance Å	No.	Atoms	Distance Å	No.	$d_\ell : d_s$
1	Li–Li	2.9343	4	Li–Li	2.9343	4	1
	Li–In	2.9343	4	Li–In	2.9343	4	
2	Li–In	3.3881	6	Li–In	3.3825	4	η
				Li–In	3.3996	2	
3	Li–Li	4.7915	12	Li–Li	4.7836	4	$\sqrt{\frac{1}{2}(1+\eta^2)}$
				Li–Li	4.7957	8	

Note. In–In distances are identical to those between Li–Li and not repeated.
The ratios between long and short distances, $d_\ell : d_s$, are expressed in terms of the tetragonal distortion $\eta = c/a\sqrt{2}$ for the split shells.

TABLE 3
Compilation of the Performed Experiments and the Obtained Results

Compound	Experiment	T/K	a (Å)	c (Å)	$c/a\sqrt{2}$	V (Å^3)	B_{iso}(Li) (Å^2)	B_{iso}(Ag,In) (Å^2)
LiIn	XRD, LR	300	4.8016(1)	6.7905(1)	1	313.11(1)		
	D2B, HR	1.5	4.7683(1)	6.7785(2)	1.0052(1)	154.12(1)	3.4(2)	0.84(5)
	D20, LR	300	4.8093(2)	6.8014(3)	1	314.63(4)	4.3(1)	1.33(3)
	D20, LR	2	4.7737(4)	6.7884(8)	1.0055(1)	154.70(3)	2.6(2)	0.45(1)
$Li_{0.97}In$	XRD, LR	300	4.7931(2)	6.7784(2)	1	311.45(2)		
	D2B, HR	1.5	4.7702(2)	6.7752(4)	1.0043(1)	154.17(2)	3.5(2)	0.8(1)
	D20, LR	300	4.8131(2)	6.8067(3)	1	315.37(3)	4.4(1)	1.61(3)
	D20, LR	2	4.7804(4)	6.7917(9)	1.0046(1)	155.20(3)	2.8(3)	0.7(1)
$Li_{1.03}In$	XRD, LR	300	4.7970(2)	6.7840(2)	1	312.21(3)		
	D20, LR	300	4.8113(2)	6.8043(3)	1	315.03(4)	3.6(1)	1.60(3)
$LiAg_{0.25}In_{0.75}$	XRD, LR	300	4.7252(2)	6.6825(3)	1	298.41(3)		
	D2B, HR	1.5	4.7023(1)	6.6501(1)	1	294.10(2)	2.2(1)	0.66(4)
$LiAg_{0.5}In_{0.5}$	XRD, LR	300	4.6503(2)	6.5765(3)	1	284.43(4)		
	D2B, HR	1.5	4.6260(2)	6.5422(2)	1	280.00(3)	1.38(5)	0.50(2)
	D2B, HR	300	4.6506(3)	6.5769(5)	1	284.49(6)	3.3(1)	2.31(4)

Note. "LR" and "HR" refer to low and high resolution, respectively. "XRD, HR" denotes an X-ray experiment as described in the text. In the case of "XRD, LR" Cu$K\alpha_1$ radiation and a curved position-sensitive detector was used. D20 and D2B are the neutron powder diffraction beamlines at ILL, Grenoble. Lattice parameters determined from X-ray and D2B data are in excellent agreement, but those obtained from D20 data differ slightly due to less precise wavelengths determination. No reliable thermal displacement parameters could be obtained from the X-ray diffraction experiments because of high absorption and low scattering power of Li.

5. CONCLUSION

LiIn is one of the seven known binary alloys with NaTl-type structure (cubic Zintl phases, B32-classification of the "Strukturberichte"). Powder diffraction using X-rays and neutrons reveal a phase transition at 170(10) K from the cubic into a tetragonal phase. The transition is reversible and "translationengleich" from spacegroup $Fd\bar{3}m$ into $I4_1/amd$. The tetragonal distortion is very small (0.50–0.55% for LiIn) and constant between the transition temperature and the lowest investigated temperature of 1.5 K. The transition takes place without a remarkable change in distances for the first coordination shell and without a significant discontinuous change in volume per formula unit. The continuity of reduced volume during this phase transition explains why this low-temperature phase is not induced at room temperature by applying pressure (8). An alloy with 3% Li deficiency shows qualitatively the same behavior, but the tetragonal distortion is smaller (0.45%). No phase transition was observed in the ternary alloys $LiAg_{0.25}In_{0.75}$ and $LiAg_{0.5}In_{0.5}$, in which In is partially and randomly replaced by silver. Therefore, silver seems to stabilize the cubic NaTl-type structure.

LiIn is the second example after NaHg for a binary Zintl phase with NaTl-type structure, stabilized at finite temperature by entropy. Compared to NaHg (9), the ground state of LiIn follows a different route of symmetry reduction into a tetragonal space group, in contrast to a rhombohedral distortion in NaHg, followed by a reconstructive phase transition into a distorted CsCl-type structured α-NaHg.

In the light of the results presented, a comprehensive reinvestigation of the low-temperature properties of all Zintl phases with NaTl-type structure appears essential to elucidate this prototypic class of compounds. The observed phase transitions in LiIn and NaHg provide severe tests for *a priori* calculations of electronic structures and predictions of crystal structures.

ACKNOWLEDGMENTS

Financial support by the *Fonds der Chemischen Industrie* and *Adolf-Messer-Stiftung* is gratefully acknowledged. This work has benefitted from allocated beamtime at the Insitute Laue-Langevin in Grenoble and travel support from the European Union in the frame of the *Human Potential Programme*. The authors thanks H. Boysen for valuable discussions.

REFERENCES

1. H. Schäfer, B. Eisenmann, and W. Müller, *Angew. Chem. Int. Ed. Engl.* **12,** 694 (1973).

2. P. C. Schmidt, *Z. Naturforsch.* **40a,** 335–346 (1985).
3. S. Kauzlarich (Ed.), "Chemistry, Structure, and Bonding of Zintl Phases and Ions," VCH Publishers, New York, 1996.
4. E. Zintl and W. Dullenkopf, *Z. Phys. Chem.* **16,** 195 (1932).
5. E. Zintl and G. Brauer, *Z. Phys. Chem.* **20,** 245 (1933).
6. H. Pauly, Thesis, TH Darmstadt, Germany, 1966.
7. H. Pauly, A. Weiss, and H. Witte, *Z. Metallk.* **59,** 47–58 (1968).
8. U. Schwartz, S. Bräuninger, K. Syassen, and R. Kniep, *J. Solid State Chem.* **137,** 104–111 (1998).
9. M. Rochnia and H.-J. Deiseroth, *Croat. Chem. Acta* **68,** 701–708 (1995).
10. H. Kezuka, *Thin Solid Films* **36**(1), 161–164 (1976).
11. H. Kezuka, *Jpn. J. Appl. Phys.* **15**(5), 895–896 (1976).
12. H. Kezuka, S. Takei, and K. Iwamura, *Proc. Int. Vac. Congr.* **7**(2), 1853–1856 (1977).
13. K. Kuriyama, H. Hamanaka, S. Kaidou, and M. Yahagi, *Phys. Rev. B* **54,** 6015–6018 (1996).
14. H. Hamanaka, S. Kaidou, K. Kuriyama, and M. Yahagi, *Solid State Ionics* **113–115,** 69–72 (1998).
15. A. C. Larson, and R. B. von Dreele, "General Structure Analysis System (GSAS)," Los Alamos National Laboratory Report LAUR 86-748, 2000.
16. J. Rodriguez-Carvajal, "FULLPROF: A Program for Rietveld Refinement and Pattern Matching Analysis," Abstracts of the Satellite Meeting on Powder Diffraction on the XV Congress of the IUCr, Toulouse, France, p. 127, 1990.
17. H. E. Schone and W. D. Knight, *Acta Metall.* **11,** 179 (1963).
18. M. Yahagi, *J. Phys. Soc. Jpn.* **43,** 2097–2098 (1977).
19. K. Kishio and J. O. Brittain, *J. Phys. Chem. Solids* **40,** 933–940 (1979).
20. T. O. Brunn and S. Susman, *Solid State Commun.* **45,** 721–724 (1983).
21. J. Schneider, *Mater. Sci. Forum* **27–28,** 63–68 (1988).
22. M. Tadin, J. Schneider, H. Boysen, and F. Frey, *Mater. Sci. Forum* **79–82,** 635–642 (1991).
23. K. Kuriyama, T. Kato, T. Kato, H. Sugai, H. Maeta, and M. Yahagi, *Phys. Rev. B* **52,** 3020–3022 (1995).
24. H. Sugai, M. Tanase, M. Yahagi, T. Ashida, H. Hamanaka, K. Kuriyama, and K. Iwamura, *Phys. Rev. B* **32,** 4050–4059 (1995).